

Infrared Spectra of the Chloromethyl and Bromomethyl Cations in Solid Argon

Renhu Ma, Mohua Chen, and Mingfei Zhou*

Department of Chemistry, Shanghai Key Laboratory of Molecular Catalysts and Innovative Materials, Advanced Materials Laboratory, Fudan University, Shanghai 200433, P. R. China

Received: September 1, 2009; Revised Manuscript Received: September 23, 2009

Infrared spectra of chloromethyl and bromomethyl cations isolated in solid argon are reported. Cocondensation of dichloromethane and dibromomethane with high-frequency discharged argon at 4 K produces the dichloromethane and dibromomethane cations, which dissociate upon visible light irradiation to form the chloromethyl and bromomethyl cations. On the basis of isotopic substitutions (^{13}C and deuterium) as well as theoretical frequency calculations, photosensitive absorptions are assigned to different vibrational modes of the chloromethyl and bromomethyl cations. Theoretical calculations predict that the halomethyl cations have a planar C_{2v} symmetry with a shorter C–X bond and longer C–H bonds relative to those of the halomethyl free radicals.

Introduction

As the halogenated derivatives of the simplest carbocation, the halomethyl cations have gained much attention. The CH_2Cl^+ and CH_2Br^+ cations have been observed in photoelectron photoion coincidence investigations on CH_2Cl_2 and CH_2Br_2 .^{1,2} The vibrational fundamentals for the ground-state CH_2Cl^+ and CH_2Br^+ cations are assigned from the photoelectron spectroscopic study on the chloromethyl and bromomethyl radicals in the gas phase.^{3,4} The C–Cl stretching vibration of CH_2Cl^+ is determined to be $1040 \pm 30 \text{ cm}^{-1}$, whereas the C–Br stretching mode of the ground-state CH_2Br^+ cation is determined to be $860 \pm 30 \text{ cm}^{-1}$. Both of the C–Cl and C–Br vibrational fundamentals are found to be substantially higher in cations than the corresponding free radicals, suggesting a substantial increase in net C–X bonding involving charge delocalization between halogen lone pairs and the carbocation center as compared with the free radicals. The bromomethyl cation has been theoretically investigated at the MP2, CCSD(T), and B3LYP levels of theory.⁵ The cation is predicted to have a planar structure with its C–Br bond length being shorter than that of neutral.

The chloromethyl and bromomethyl cations are the lowest-energy decomposition products of the dichloromethane and dibromomethane cations and are the major fragments observed in the gas-phase mass spectrometric studies. However, neither cation has been observed in previous matrix isolation spectroscopic investigations on the neutral and ionic decomposition products of dihalomethanes.^{6,7} The absence of chloromethyl and bromomethyl cations in solid noble gas matrixes has been proposed to be due to either their extremely weak infrared absorptions or the very efficient neutralization of these species in rare-gas matrices.⁷ The vibrational frequencies of chloromethyl and bromomethyl cations have not been reported in the gas phase except the C–Cl and C–Br stretching vibrations. In this article, we report a combined matrix isolation infrared absorption spectroscopic and theoretical study of halomethyl cations, which are produced via the dissociation of dihalomethane cations in solid argon.

Experimental and Computational Methods

The halomethyl cations are prepared by high-frequency discharge in conjunction with matrix isolation technique, which has proven to be an effective method in producing and trapping unstable species for spectroscopic study.^{8–12} The experimental setup for high-frequency discharge and matrix isolation Fourier transform infrared spectroscopic investigation has previously been described in detail.¹³ In brief, a pure argon gas stream is subjected to discharge from a high-frequency generator (Tesla coil, alternating voltage ranging from 0 to 9 kV and frequency ranging from 10 to 15 kHz). The resulting beam is mixed with another gas stream containing CH_2X_2 (X = Cl, Br)/Ar mixture outside the discharge region, followed by codeposition on the surface of a CsI window cooled normally to 4 K by means of a closed-cycle helium refrigerator. In general, matrix samples are deposited for 1 h at a rate of $\sim 5 \text{ mmol/h}$ for each stream. The infrared absorption spectra of the resulting samples are recorded on a Bruker Vertex 80v spectrometer at 0.5 cm^{-1} resolution between 4000 and 450 cm^{-1} using a DTGS detector. After the infrared spectrum of the initial deposit has been recorded, the sample is annealed to different temperatures and cooled back to 4 K for spectral acquisition. Selected samples are also subjected to broadband irradiation using a tungsten lamp with glass filters. The CH_2X_2 (X = Cl, Br)/Ar (1:1000) mixtures are prepared in a stainless steel vacuum line using standard manometric technique. $^{13}\text{CH}_2\text{Cl}_2$ (Aldrich, 99%), CD_2Cl_2 (Aldrich, 99%), and CD_2Br_2 (Aldrich, 99%) are used without further purification in different experiments.

Quantum chemical calculations are performed using the Gaussian 03 program.¹⁴ The three-parameter hybrid functional according to Becke with additional correlation corrections due to Lee, Yang, and Parr (B3LYP) is utilized.¹⁵ The 6-311++G** basis set is used for the H, C, Cl, and Br atoms.¹⁶ The geometries are fully optimized; the harmonic vibrational frequencies are calculated, and zero-point vibrational energies (ZPVEs) are derived.

Results and Discussion

Infrared Spectra. The infrared spectra obtained from cocondensation of dichloromethane/argon mixture with high-

* Corresponding author. E-mail: mfzhou@fudan.edu.cn.

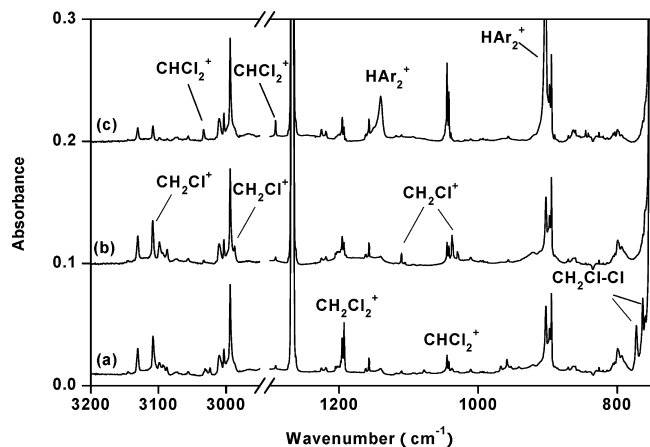


Figure 1. Infrared spectra in the 3200–2950 and 1300–750 cm^{-1} regions from codeposition of 0.1% $\text{CH}_2\text{Cl}_2/\text{Ar}$ with high-frequency discharged Ar: (a) after 1 h of sample deposition at 4 K, (b) after 15 min of $\lambda > 500$ nm irradiation, and (c) after 15 min of broadband irradiation ($250 < \lambda < 580$ nm).

frequency discharged argon at 4 K reveal that the products due to fragmentation of precursor are relatively more abundant with high power of discharge, whereas the species considered to be from isomerization of precursor are favored with low power of discharge. Figure 1 shows the spectra in selected regions from co-condensation of 0.1% dichloromethane in argon with high-frequency discharged argon using relatively low power of discharge. After 1 h of sample deposition at 4 K, a series of product absorptions are observed. The 3029.3/3023.7, 1408.0/1405.1, 967.5, 958.6/952.8, and 772.5/763.2 cm^{-1} absorptions are attributed to isodichloromethane, which has previously been characterized by infrared and UV–visible spectroscopic studies of the photoisomerization of dichloromethane in solid argon.¹⁷ The 1192.8 cm^{-1} absorption corresponding to the absorption reported at 1193 cm^{-1} has previously been assigned to the parent CH_2Cl_2^+ ion.^{6,7} The 3108.2 and 2881.8 cm^{-1} absorptions correspond to the absorptions previously assigned to the $\text{HCICl}-\text{Cl}-\text{H}^+$ cation.⁷ The 2904.1 and 3130.8 cm^{-1} absorptions have previously been attributed to the $(\text{CH}_2\text{Cl}^+)\text{Cl}$ complex.⁷ Besides the above-mentioned species, fragmentation species including CH_2Cl (1390.0, 826.1, and 820.1 cm^{-1}), CHCl_2^+ (3033.4, 1291.3, 1044.7/1042.0/1039.2, 845.3/841.4/837.7 cm^{-1}), and CCl_2^+ (1195.5/1192.9/1190.2 cm^{-1}) are also observed.^{18–20} Both the isodichloromethane and CH_2Cl_2^+ absorptions decrease in intensity when the as-deposited sample is subjected to visible light irradiation using a tungsten lamp with a 500 nm long-wavelength pass filter, during which a group of new absorptions at 3109.3, 2987.3, 1110.2, 1037.6, and 1029.7 cm^{-1} are produced. (The 3109.3 cm^{-1} absorption is overlapped by the $\text{HCICl}-\text{Cl}-\text{H}^+$ absorption at 3108.2 cm^{-1} but can be clearly resolved in the difference spectrum.) The other species mentioned above remain unchanged upon $\lambda > 500$ nm irradiation. The 3109.3, 2987.3, 1110.2, 1037.6, and 1029.7 cm^{-1} absorptions disappear upon subsequent broadband UV–visible irradiation with a high-pressure mercury lamp ($250 < \lambda < 580$ nm). The absorptions due to $\text{HCICl}-\text{Cl}-\text{H}^+$ and $(\text{CH}_2\text{Cl}^+)\text{Cl}$ decrease, whereas the CHCl_2^+ absorptions markedly increase in intensity under UV–visible irradiation. The HAr_2^+ absorptions (1139.7 and 903.1 cm^{-1}) are also produced.²¹ The difference spectra illustrated in Figure 2 show more clearly the behavior of the product absorptions under different wavelength range irradiations. A similar experiment has been done focusing on annealing, which shows that the 3109.3, 2987.3, 1110.2, 1037.6, and 1029.7 cm^{-1} absorptions produced on $\lambda > 500$ nm

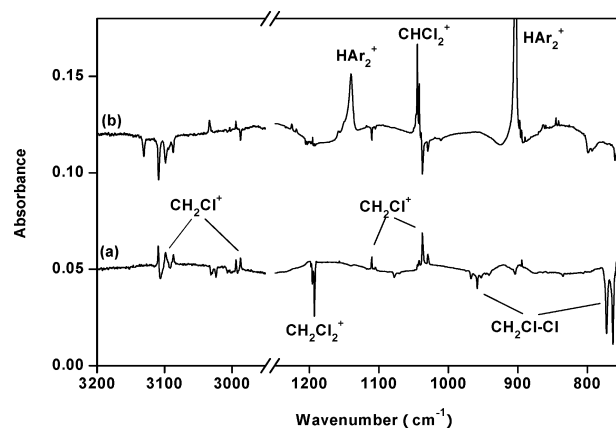


Figure 2. Difference IR spectra in the 3200–2950 and 1250–750 cm^{-1} regions from codeposition of 0.1% $\text{CH}_2\text{Cl}_2/\text{Ar}$ with high-frequency discharged Ar: (a) spectrum taken after 15 min of $\lambda > 500$ nm irradiation minus spectrum taken right after 1 h of sample deposition at 4 K and (b) spectrum taken after 15 min of UV–visible irradiation ($250 < \lambda < 580$ nm) minus spectrum taken after 15 min of $\lambda > 500$ nm irradiation.

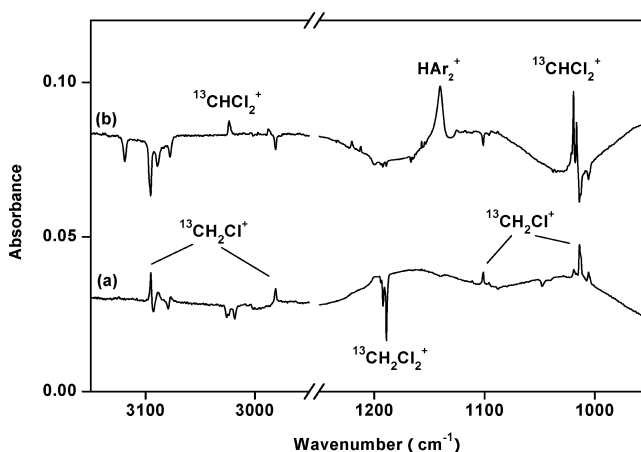


Figure 3. Difference IR spectra in the 3150–2950 and 1250–950 cm^{-1} regions from codeposition of 0.1% $^{13}\text{CH}_2\text{Cl}_2/\text{Ar}$ with high-frequency discharged Ar: (a) spectrum taken after 15 min of $\lambda > 500$ nm irradiation minus spectrum taken right after 1 h of sample deposition at 4 K and (b) spectrum taken after 15 min of UV–visible irradiation ($250 < \lambda < 580$ nm) minus spectrum taken after 15 min of $\lambda > 500$ nm irradiation.

irradiation are also very sensitive on annealing. These absorptions disappear when the sample is annealed above 20 K. It has been found that the CH_2Cl_2^+ absorption is partially recovered with the disappearance of the 3109.3, 2987.3, 1110.2, 1037.6, and 1029.7 cm^{-1} absorptions on annealing. The experiments have been repeated with the isotopic-labeled $\text{CD}_2\text{Cl}_2/\text{Ar}$ and $^{13}\text{CH}_2\text{Cl}_2/\text{Ar}$ samples; the infrared spectra in selected regions are shown in Figures 3 and 4, respectively. The deuterium and carbon-13 isotopic counterparts of the newly observed absorptions are listed in Table 1.

Similar experiments have also been performed with a dibromomethane/Ar sample. The infrared spectra from codeposition of dibromomethane/Ar with high-frequency discharged argon are shown in Figure 5, and the difference spectra in selected regions are illustrated in Figure 6. After 1 h of sample deposition, the isodibromomethane absorptions (684.7 and 694.8 cm^{-1}) are observed to be the major product.¹⁷ The previously characterized CH_2Br (1355.1, 952.4, and 693.2 cm^{-1}), CHBr_2 (1164.6 and 778.4 cm^{-1}), and CHBr_2^+ (1227.3 and 896.9 cm^{-1}) absorptions^{6,7} together with a group of absorptions at 3099.4,

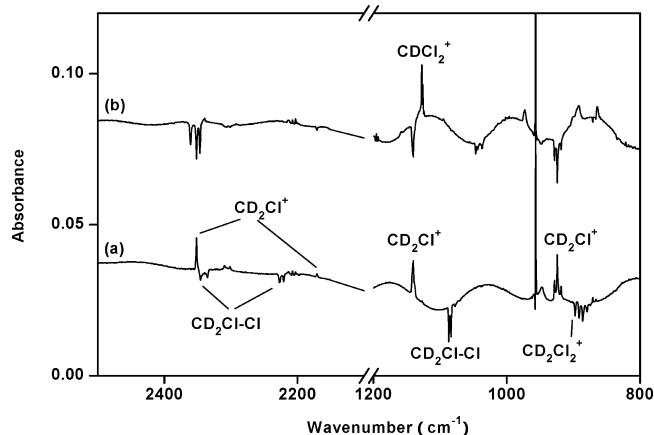


Figure 4. Difference IR spectra in the 2500–2100 and 1200–800 cm^{-1} regions from codeposition of 0.1% $\text{CD}_2\text{Cl}_2/\text{Ar}$ with high-frequency discharged Ar: (a) spectrum taken after 15 min of $\lambda > 500$ nm irradiation minus spectrum taken right after 1 h of sample deposition at 4 K and (b) spectrum taken after 15 min of UV–visible irradiation ($250 < \lambda < 580$ nm) minus spectrum taken after 15 min of $\lambda > 500$ nm irradiation.

1128.1, and 525.3 cm^{-1} are also observed. The isodibromomethane absorptions as well as the 3099.4, 1128.1, and 525.3 cm^{-1} absorptions are destroyed under visible light irradiation, whereas a set of new absorptions at 3127.9, 2998.8, 1024.8, and 863.7 cm^{-1} are produced. The 3099.4, 1128.1, and 525.3 cm^{-1} absorptions are recovered, whereas the 3127.9, 2998.8, 1024.8, and 863.7 cm^{-1} absorptions disappear under subsequent broadband UV–visible irradiation. The CH_2Br , CHBr_2 , and CHBr_2^+ absorptions are unaffected by different wavelength range irradiations. The experiment has been repeated using the deuterium substituted sample. The 3099.4, 1128.1, and 525.3 cm^{-1} absorptions in the CH_2Br_2 experiment shift to 2341.8, 849.1, and 506.0 cm^{-1} when CD_2Br_2 is used. Absorptions at 2366.4, 2209.7, 1075.6, 801.8, and 791.1 cm^{-1} produced on visible light irradiation are the counterparts of the 3127.9, 2998.8, 1024.8, and 863.7 cm^{-1} absorptions in the CH_2Br_2 experiment. The 1128.1 cm^{-1} absorption corresponds to the absorption reported at 1129 cm^{-1} , which has previously been assigned to the CH_2Br_2^+ cation.⁶ In the previous report, absorptions at 685 and 695 cm^{-1} (corresponding to the absorptions at 684.7 and 694.8 cm^{-1} in this study) have also been attributed to the CH_2Br_2^+ cation. These absorptions have been reassigned to isodibromomethane.¹⁷ In the present study, the absorptions at 3099.4 and 525.3 cm^{-1} track with the 1128.1 cm^{-1} absorption and are due to the CH_2 stretching and CBr_2 stretching vibrations of the CH_2Br_2^+ cation in solid argon. The band positions of the newly observed species together with their deuterium counterparts are listed in Table 2.

CH_2Cl^+ . On the basis of the consistent behavior in different samples, absorptions at 3109.3, 2987.3, 1110.2, 1037.6, and 1029.7 cm^{-1} can be grouped together as vibrational modes of the same species. The 3109.3 and 2987.3 cm^{-1} absorptions shift to 3095.1 and 2981.0 cm^{-1} when a $^{13}\text{CH}_2\text{Cl}_2/\text{Ar}$ sample is used and shift to 2351.5 and 2171.0 cm^{-1} in the experiment using a $\text{CD}_2\text{Cl}_2/\text{Ar}$ sample. The band positions and isotopic shifts imply that these two absorptions are due to CH stretching modes and that the absorber involves one CH_2 subunit. The 1037.6 and 1029.7 cm^{-1} absorptions in the $\text{CH}_2\text{Cl}_2/\text{Ar}$ experiments exhibit the appropriate relative infrared intensities for isotopic splittings of one chlorine atom in natural abundance ($^{35}\text{Cl}/^{37}\text{Cl} = 0.76:0.24$). The isotopic shifts indicate that these two absorptions are due to the C–Cl stretching vibrations. The 1110.2 cm^{-1}

absorption shows no chlorine isotopic shift and is due to a CH_2 wagging vibration. The above-mentioned spectral features indicate that the absorber has a CH_2Cl stoichiometry. The photosensitive behavior of these absorptions suggests that the absorber is likely due to a charged species. Note that the observed C–Cl stretching vibration is very close to those of the chlorine-containing cations, such as CHCl_2^+ and CHCl^+ , but is >200 cm^{-1} higher than that of the CH_2Cl radical.^{18–20} Accordingly, we assign the 3109.3, 2987.3, 1110.2, 1037.6, and 1029.7 cm^{-1} absorptions to the CH_2Cl^+ cation isolated in solid argon (Table 1). The 2351.5, 2171.0, 1140.5, 924.2, and 918.4 cm^{-1} absorptions observed in the $\text{CD}_2\text{Cl}_2/\text{Ar}$ experiments are assigned to the CD_2Cl^+ cation. The C–Cl stretching vibration of CH_2Cl^+ in the gas phase has been determined to be 1040 ± 30 cm^{-1} ,³ which is in excellent agreement with the value observed in solid argon.

Theoretical calculations have been performed on the CH_2Cl^+ cation to support the assignment. For comparison, the CH_2Cl free radical is also calculated. The optimized structures are shown in Figure 7, and the vibrational frequencies and intensities are listed in Table 1. The CH_2Cl^+ cation is predicted to have a $^1\text{A}_1$ ground state with a planar C_{2v} symmetry. The calculated C–H bond length of the cation is longer, whereas the C–Cl bond length is shorter than those of the CH_2Cl free radical calculated at the same level of theory. As shown in Figure 8, the singly occupied molecular orbital (SOMO) of the chloromethyl radical is an antibonding π orbital, which consists of the 2p atomic orbital of carbon and the 3p atomic orbital of chlorine. Removing one electron from this orbital results in the singlet ground state CH_2Cl^+ cation. Because the SOMO of the CH_2Cl radical is C–Cl antibonding in character, detaching one electron from this orbital strengthens the C–Cl bond to give a shorter C–Cl bond length.

The CH_2Cl^+ cation with C_{2v} symmetry possesses six vibrational modes, and all are expected to be IR active. Four of the six fundamental absorptions are observed experimentally. These modes are predicted to be 3221.2, 3081.6, 1155.8, and 1045.2 cm^{-1} with 48, 17, 30, and 97 km/mol IR intensities. The calculated band positions, relative intensities, and isotopic frequency shifts fit the experimental values very well (Table 1). The CH_2 scissoring and CH_2 rocking modes are predicted to have very low IR intensities (<1 km/mol) and are not observed experimentally. For the CD_2Cl^+ cation, five modes are predicted to have appreciable IR intensities, which are experimentally observed. The CH_2 scissoring mode, which is predicted to have very low IR intensity, is greatly intensified with deuterium substitution.

CH_2Br^+ . The absorptions at 3127.9, 2998.7, 1024.7, and 863.7 cm^{-1} in the CH_2Br_2 experiments are assigned to the CH_2Br^+ cation following the example of CH_2Cl^+ . The absorptions at 3127.9 and 2998.7 cm^{-1} are due to the antisymmetric and symmetric CH_2 stretching vibrations. The absorption at 863.7 cm^{-1} is due to the C–Br stretching vibration, which is in excellent agreement with the gas-phase value of 860 ± 30 cm^{-1} determined by photoelectron spectroscopy.⁴ The 1024.7 cm^{-1} absorption is attributed to the CH_2 wagging vibration, which is ~ 85.5 cm^{-1} lower than that of the CH_2Cl^+ cation. In the experiment with a CD_2Br_2 sample, five absorptions are observed. The two CD_2 stretching modes are observed at 2366.3 and 2209.6 cm^{-1} . The C–Br stretching mode shifts to 791.1 cm^{-1} upon deuterium substitution. The CH_2 wagging vibration is observed at 801.8 cm^{-1} . Besides the modes observed in the CH_2Br_2 experiments, an additional absorption at 1075.6 cm^{-1}

TABLE 1: Comparison between the Calculated and Observed Vibrational Frequencies (inverse centimeters) and Intensities (in Parentheses) for the CH_2Cl^+ Cation

calcd ^a			exptl ^b			mode
$^{12}\text{CH}_2\text{Cl}^+$	$^{12}\text{CD}_2\text{Cl}^+$	$^{13}\text{CH}_2\text{Cl}^+$	$^{12}\text{CH}_2\text{Cl}^+$	$^{12}\text{CD}_2\text{Cl}^+$	$^{13}\text{CH}_2\text{Cl}^+$	
3221.2(48)	2410.8(17)	3206.5(49)	3109.3(0.62)	2351.5(0.52)	3095.1(0.65)	CH asym. str.
3081.6(17)	2232.0(2)	3076.5(19)	2987.3(0.34)	2170.9(0.03)	2981.1(0.29)	CH sym. str.
1481.1(0.1)	1165.0(34)	1474.0(0.5)		1140.4(0.74)		CH_2 scis.
1155.8(30)	907.8(8)	1145.5(31)	1110.2(0.29)	871.0(0.08)	1101.1(0.21)	CH_2 wag
1061.2(0.4)	807.8(0.2)	1055.3(0.6)				CH_2 rock
1045.2(97)	936.7(52)	1021.0(90)	1037.6(1.00)	924.3(1.00)	1013.8(1.00)	C^{35}Cl str.
1037.1(98)	930.4(54)	1012.6(90)	1029.7(0.27)	918.4(0.28)	1005.6(0.32)	C^{35}Cl str.

^a In kilometers per mole. ^b Integrated intensity normalized to the most intense absorption.

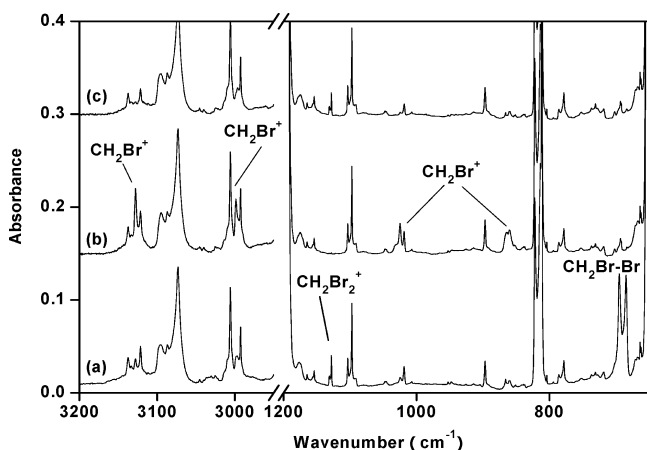


Figure 5. Infrared spectra in the 3200–2950 and 1200–650 cm^{-1} regions from codeposition of 0.1% $\text{CH}_2\text{Br}_2/\text{Ar}$ with high-frequency discharged Ar: (a) after 1 h of sample deposition at 4 K, (b) after 15 min of $\lambda > 500$ nm irradiation, and (c) after 15 min of broadband irradiation ($250 < \lambda < 580$ nm).

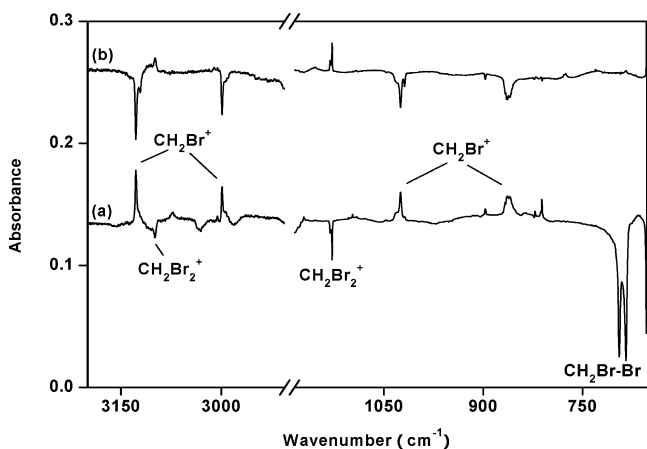


Figure 6. Difference IR spectra in the 3200–2950 and 1200–650 cm^{-1} regions from codeposition of 0.1% $\text{CH}_2\text{Br}_2/\text{Ar}$ with high-frequency discharged Ar: (a) spectrum taken after 15 min of $\lambda > 500$ nm irradiation minus spectrum taken right after 1 h of sample deposition at 4 K, and (b) spectrum taken after 15 min of UV–visible irradiation ($250 < \lambda < 580$ nm) minus spectrum taken after 15 min of $\lambda > 500$ nm irradiation.

is also observed with deuterium substitution, which is assigned to the CD_2 scissoring vibration.

The CH_2Br^+ is predicted to have a $^1\text{A}_1$ ground state with a planar C_{2v} symmetry, which is in agreement with previous theoretical calculations.⁵ As shown in Figure 7, the C–Br and C–H bond lengths are predicted to be 0.108 Å shorter and 0.011 Å longer than those of the CH_2Br radical. The calculated vibrational frequencies and intensities of CH_2Br^+ and CD_2Br^+

TABLE 2: Comparison between the Calculated and Observed Vibrational Frequencies (inverse centimeters) and Intensities (in Parentheses) for the CH_2Br^+ Cation

calcd ^a		exptl ^b		mode
CH_2Br^+	CD_2Br^+	CH_2Br^+	CD_2Br^+	
3225.5(50)	2420.2(20)	3127.9(1.00)	2366.3(1.00)	CH asym. str.
3093.2(26)	2237.8(5)	2998.7(0.79)	2209.6(0.17)	CH sym. str.
1450.2(0)	1106.0(13)		1075.6(0.31)	CH_2 scis.
1095.6(37)	857.1(12)	1024.7(0.59)	801.8(0.81)	CH_2 wag
982.9(2)	737.5(2)			CH_2 rock
861.3(73)	798.5(53)	863.7(0.94)	791.1(0.97)	CBr str.

^a In kilometers per mole. ^b Integrated intensity normalized to the most intense absorption.

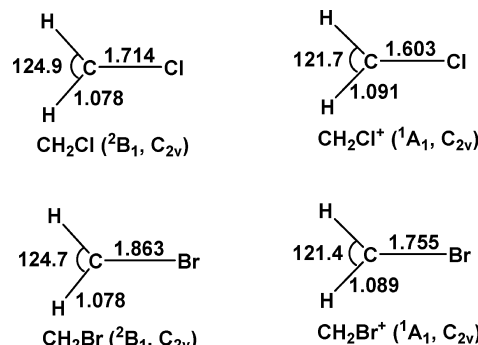


Figure 7. Optimized structures (bond lengths in angstroms; bond angles in degrees) of CH_2X^+ and CH_2X ($\text{X} = \text{Cl}, \text{Br}$).

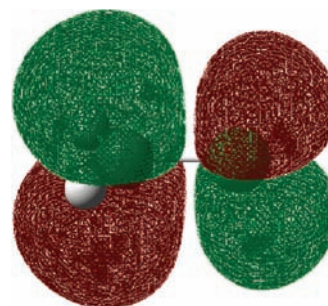
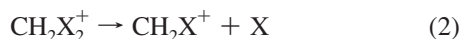
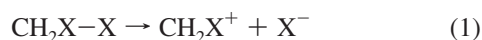


Figure 8. Three-dimensional contours of the singly occupied molecular orbital (SOMO) of CH_2X .

are listed in Table 2. Both the band positions and relative intensities match the experimental observations very well.

Reaction Mechanism. Cocondensation of CH_2X_2 ($\text{X} = \text{Cl}, \text{Br}$)/Ar with high-frequency discharged argon produces the isodihalomethane $\text{CH}_2\text{X}-\text{X}$ and parent ions CH_2X_2^+ as the major products. In addition, some fragmentation species are also observed. The CH_2X^+ cations are formed upon visible light irradiation, during which only the isodihalomethane and CH_2X_2^+ cation absorptions decrease in intensity. This observation implies that the CH_2X^+ cations can be formed via two possible

mechanisms: photoinduced electron transfer decomposition of isodihalomethane (reaction 1) and photoinduced dissociation of parent CH_2X_2^+ ion (reaction 2)



On the basis of theoretical calculations, reaction 1 is predicted to be highly endothermic (~ 130 kcal/mol for both the Cl and Br systems); therefore, the mechanism for the formation of CH_2X^+ cations from isodihalomethane can be ruled out. As has been discussed, the CH_2X^+ cations are extremely facile in the gas phase.^{1,2} Although the absorption maximum appears in the UV region, both cations absorb continuously and photodissociate in the visible range.⁶ The lowest energy ion dissociation product for both of the methylene halide cations is that to form CH_2X^+ . The threshold energy for this X-atom detachment to occur for both of the systems studied is ~ 0.8 eV.^{1,2,6} However, additional energy is needed to effect this detachment for a matrix-isolated deposit to form the exiting halogen atom with sufficient kinetic energy for it to escape the "cage" in which it is formed.

The CH_2X^+ cation absorptions are very sensitive to annealing. Both the CH_2Cl^+ and CH_2Br^+ cation absorptions disappear on sample annealing, during which the parent CH_2X_2^+ absorptions increase. Because of the matrix cage effect, the CH_2X^+ and X photoproducts of reaction 2 are unable to escape the matrix cage and are trapped in the same matrix cage. Therefore, the CH_2X^+ cations are able to recombine with the X atoms to form the CH_2X_2^+ cations on annealing. The CH_2X^+ cation absorptions are also sensitive to UV irradiation. In the CH_2Cl_2 system, the CHCl_2^+ and HAr_2^+ cation absorptions are produced with the disappearance of the CH_2Cl^+ absorption under UV-visible irradiation ($250 < \lambda < 580$ nm). It implies that the UV-visible photons cause the reaction of the CH_2Cl^+ cation with the chlorine atom trapped in the same matrix cage to give the CHCl_2^+ and HAr_2^+ cations. In the CH_2Br_2 system, the CHBr_2^+ cation absorptions remain unchanged, and no HAr_2^+ absorptions are produced upon UV-visible irradiation. In contrast, the CH_2Br_2^+ absorptions are found to increase at the expense of the CH_2Br^+ absorptions. Apparently, the CH_2Br^+ cation prefers to react with the Br atom trapped in the same matrix cage to form the CH_2Br_2^+ cation.

The CH_2X^+ cations have not been observed in previous matrix isolation spectroscopic studies.^{6,7} It has been assumed that these ionic species are present but in quantities that are not observable by the relatively insensitive infrared spectroscopy or that the electron affinities for these species are too high to be stabilized in solid argon.^{6,7} As has been pointed out, any attempts to isolate cations are unsuccessful when there is < 5 eV difference between the ionization potential of the matrix substrate atom and the electron affinity of the cation.²² There is no experimental report on the ionization energies of CH_2Cl and CH_2Br . These ionization energies are expected to be lower than or comparable to those of a number of other species such as CCl_3 and HCCl_2 . The CCl_3^+ and HCCl_2^+ cations have been stabilized in solid argon.^{19a,23} Note that previous matrix isolation experiments are performed in argon matrix at 15 K,^{6,7} whereas the present experiments are done at 4 K. As has been mentioned above, the CH_2X^+ cations are very sensitive to annealing, and the cation absorptions disappear on sample annealing. We propose that

the cations are unable to be stabilized in argon matrix at 15 K. (The temperature on sample may be even higher during visible irradiation.)

Conclusions

Cocondensation of CH_2X_2 ($\text{X} = \text{Cl}, \text{Br}$)/Ar with high-frequency discharged argon produces the isodihalomethane $\text{CH}_2\text{X}-\text{X}$ complexes and the parent ions CH_2X_2^+ as the major products. Under visible light irradiation, the CH_2X_2^+ cations dissociate to give the halomethyl cations CH_2X^+ . Four of the six vibrational fundamentals of the CH_2X^+ cations are observed, and five vibrational fundamentals are observed for the CD_2X^+ cations. The halomethyl cations are predicted to have a planar C_{2v} symmetry with a shorter C-X bond and longer C-H bonds relative to those of the halomethyl free radicals. The CH_2X^+ cation absorptions are sensitive to UV-visible irradiation and sample annealing. The CH_2X^+ and X photoproducts trapped in the sample matrix cage recombine to form the CH_2X_2^+ cations on annealing. Under UV-visible irradiation, the CH_2Cl^+ cation reacts with the Cl atom, resulting in the formation of the CHCl_2^+ and HAr_2^+ cations, whereas the CH_2Br^+ cation interacts with the Br atom to form the CH_2Br_2^+ cation.

Acknowledgment. We gratefully acknowledge financial support from the National Basic Research Program of China (grant no. 2007CB815203) and the National Natural Science Foundation of China (grant no. 20773030).

References and Notes

- (1) Werner, A. S.; Tsai, B. P.; Baer, T. *J. Chem. Phys.* **1974**, *60*, 3650.
- (2) Tsai, B. P.; Baer, T.; Werner, A. S.; Lin, S. F. *J. Phys. Chem.* **1975**, *79*, 570.
- (3) (a) Andrews, L.; Dyke, J. M.; Jonathan, N.; Keddar, N.; Morris, A.; Ridha, A. *Chem. Phys. Lett.* **1983**, *97*, 89. (b) Andrews, L.; Dyke, J. M.; Jonathan, N.; Keddar, N.; Morris, A. *J. Am. Chem. Soc.* **1984**, *106*, 299.
- (4) Andrews, L.; Dyke, J. M.; Jonathan, N.; Keddar, N.; Morris, A. *J. Phys. Chem.* **1984**, *88*, 1950.
- (5) Li, Z. J.; Francisco, J. S. *J. Chem. Phys.* **1999**, *110*, 817.
- (6) Andrews, L.; Prochaska, T.; Ault, B. S. *J. Am. Chem. Soc.* **1979**, *101*, 9.
- (7) Fridgen, T. D.; Zhang, X. K.; Parnis, J. M.; March, R. E. *J. Phys. Chem. A* **2000**, *104*, 3487.
- (8) (a) Jacox, M. E. *Rev. Chem. Intermed.* **1978**, *2*, 1. (b) Jacox, M. E. In *Chemistry and Physics of Matrix-Isolated Species*; Andrews, L., Moskovits, M., Eds.; North-Holland: Amsterdam, 1989.
- (9) Bohn, R. B.; Hannachi, Y.; Andrews, L. *J. Am. Chem. Soc.* **1992**, *114*, 6452.
- (10) Langford, V. S.; McKinley, A. J.; Quickenden, T. I. *J. Am. Chem. Soc.* **2000**, *122*, 12859.
- (11) (a) Zhou, M. F.; Zeng, A. H.; Wang, Y.; Kong, Q. Y.; Wang, Z. X.; Schleyer, P. R. *J. Am. Chem. Soc.* **2003**, *125*, 11512. (b) Zeng, A. H.; Yu, L.; Wang, Y.; Kong, Q. Y.; Xu, Q.; Zhou, M. F. *J. Phys. Chem. A* **2004**, *108*, 6656. (c) Yu, L.; Zeng, A. H.; Xu, Q.; Zhou, M. F. *J. Phys. Chem. A* **2004**, *108*, 8264. (d) Zhou, H.; Yang, R. J.; Jin, X.; Zhou, M. F. *J. Phys. Chem. A* **2005**, *109*, 6003. (e) Zhou, H.; Gong, Y.; Zhou, M. F. *J. Phys. Chem. A* **2007**, *111*, 603.
- (12) (a) Yang, R. J.; Yu, L.; Zeng, A. H.; Zhou, M. F. *J. Phys. Chem. A* **2004**, *108*, 4228. (b) Yang, R. J.; Yu, L.; Jin, X.; Zhou, M. F.; Carpenter, B. K. *J. Chem. Phys.* **2005**, *122*, 014511.
- (13) (a) Ma, R. H.; Yuan, D. M.; Chen, M. H.; Zhou, M. F. *J. Phys. Chem. A* **2009**, *113*, 1250. (b) Wang, G. J.; Zhou, M. F. *Int. Rev. Phys. Chem.* **2008**, *27*, 1.
- (14) Frisch, M. J.; Trucks, G. W.; Schlegel, H. B.; Scuseria, G. E.; Robb, M. A.; Cheeseman, J. R.; Montgomery, J. A., Jr.; Vreven, T.; Kudin, K. N.; Burant, J. C.; Millam, J. M.; Iyengar, S. S.; Tomasi, J.; Barone, V.; Mennucci, B.; Cossi, M.; Scalmani, G.; Rega, N.; Petersson, G. A.; Nakatsuji, H.; Hada, M.; Ehara, M.; Toyota, K.; Fukuda, R.; Hasegawa, J.; Ishida, M.; Nakajima, T.; Honda, Y.; Kitao, O.; Nakai, H.; Klene, M.; Li, X.; Knox, J. E.; Hratchian, H. P.; Cross, J. B.; Adamo, C.; Jaramillo, J.; Gomperts, R.; Stratmann, R. E.; Yazyev, O.; Austin, A. J.; Cammi, R.; Pomelli, C.; Ochterski, J. W.; Ayala, P. Y.; Morokuma, K.; Voth, G. A.; Salvador, P.; Dannenberg, J. J.; Zakrzewski, V. G.; Dapprich, S.; Daniels, A. D.; Strain, M. C.; Farkas, O.; Malick, D. K.; Rabuck, A. D.; Raghavachari, K.; Foresman, J. B.; Ortiz, J. V.; Cui, Q.; Baboul, A. G.;

Clifford, S.; Cioslowski, J.; Stefanov, B. B.; Liu, G.; Liashenko, A.; Piskorz, P.; Komaromi, I.; Martin, R. L.; Fox, D. J.; Keith, T.; Al-Laham, M. A.; Peng, C. Y.; Nanayakkara, A.; Challacombe, M.; Gill, P. M. W.; Johnson, B.; Chen, W.; Wong, M. W.; Gonzalez, C.; Pople, J. A. *Gaussian 03*, revision B.05; Gaussian, Inc.: Pittsburgh, PA, 2003.

(15) (a) Becke, A. D. *J. Chem. Phys.* **1993**, *98*, 5648. (b) Lee, C.; Yang, W.; Parr, R. G. *Phys. Rev. B* **1988**, *37*, 785.

(16) (a) McLean, A. D.; Chandler, G. S. *J. Chem. Phys.* **1980**, *72*, 5639.

(b) Krishnan, R.; Binkley, J. S.; Seeger, R.; Pople, J. A. *J. Chem. Phys.* **1980**, *72*, 650.

(17) Maier, G.; Reisenauer, H. P.; Hu, J.; Schaad, L. J.; Hess, B. A., Jr. *J. Am. Chem. Soc.* **1990**, *112*, 5117.

(18) Kelsall, B. J.; Andrews, L. *J. Mol. Spectrosc.* **1983**, *97*, 362.

(19) (a) Jacox, M. E.; Milligan, D. E. *J. Chem. Phys.* **1971**, *54*, 3935.

(b) Jacox, M. E.; Milligan, D. E. *J. Chem. Phys.* **1970**, *53*, 2688. (c) Jacox, M. E.; Milligan, D. E. *J. Chem. Phys.* **1967**, *47*, 1626.

(20) Andrews, L.; Smith, D. W. *J. Chem. Phys.* **1970**, *53*, 2956.

(21) (a) Bondybey, V. E.; Pimentel, G. C. *J. Chem. Phys.* **1972**, *56*, 3832. (b) Milligan, D. E.; Jacox, M. E. *J. Mol. Spectrosc.* **1973**, *46*, 460.

(c) Wight, C. A.; Ault, B. S.; Andrews, L. *J. Chem. Phys.* **1976**, *65*, 1244.

(22) (a) Knight, L. B., Jr. *Acc. Chem. Res.* **1996**, *19*, 313. (b) Knight, L. B., Jr.; Kerr, K.; Villanueva, M.; McKinley, A. J.; Feller, D. *J. Chem. Phys.* **1992**, *97*, 5363.

(23) Jacox, M. E. *Chem. Phys.* **1976**, *12*, 51.

JP9084266